

Short communication

# Ce<sub>0.8</sub>Gd<sub>0.2</sub>O<sub>2-δ</sub> ceramics derived from commercial submicron-sized CeO<sub>2</sub> and Gd<sub>2</sub>O<sub>3</sub> powders for use as electrolytes in solid oxide fuel cells

J. Ma<sup>a</sup>, T.S. Zhang<sup>a,\*</sup>, L.B. Kong<sup>a</sup>, P. Hing<sup>a</sup>, S.H. Chan<sup>b</sup>

<sup>a</sup> School of Materials Engineering, Nanyang Technological University, Nanyang Avenue, Singapore 639798, Singapore

<sup>b</sup> School of Mechanical and Production Engineering, Nanyang Technological University, Nanyang Avenue, Singapore 639798, Singapore

Received 29 August 2003; accepted 22 December 2003

## Abstract

Twenty percentage of Gd<sub>2</sub>O<sub>3</sub>-doped ceria solid solution has been prepared as an electrolyte for solid oxide fuel cells via the conventional mixed-oxide method from high-purity commercial CeO<sub>2</sub> and Gd<sub>2</sub>O<sub>3</sub>. The solubility of Gd<sub>2</sub>O<sub>3</sub> in CeO<sub>2</sub> in the temperature range of 1300–1700 °C has been examined based on the measurements of the lattice parameter. It is found that the dissolution of Gd<sub>2</sub>O<sub>3</sub> in CeO<sub>2</sub> is completed at 1600 °C for 5 h. The addition of Gd<sub>2</sub>O<sub>3</sub> increases sintering temperature, retards densification, and also depresses grain growth as compared with undoped CeO<sub>2</sub>. The sample sintered at 1550 °C for 5 h has the highest grain boundary conductivity, while the highest grain interior conductivity is achieved for the sample sintered at 1600 °C for 5 h. It is also observed that below 500 °C, the maximum total conductivity is exhibited by the former sample, but above 500 °C, for the latter one.

© 2004 Elsevier B.V. All rights reserved.

**Keywords:** Cerium oxide; Gadolinium oxide; Ceramic electrolyte; Sintering; Electrical properties; Solid oxide; Fuel cell

## 1. Introduction

Two major advantages of solid oxide fuel cell (SOFC) systems are high efficiency and very low emission of pollutants. To date, yttria-stabilised zirconia (YSZ) has been mainly used as the solid oxide electrolyte for such fuel cells because of its nearly pure oxygen ionic conductivity in an oxidising or a reducing atmosphere and its good mechanical properties. To maintain high oxygen ionic conductivity, however, high operating temperatures of over 900 °C are required for this electrolyte. This condition increases the fabrication cost and accelerates degradation of the fuel-cell system.

Ceria-based solid solutions have been regarded as the most promising electrolytes for intermediate temperature (500–600 °C) SOFC (IT-SOFC) systems because their ionic conductivity is higher than that of YSZ. The ionic conductivity of ceria has been extensively investigated with respect to different dopants (e.g., Ca<sup>2+</sup>, Sr<sup>2+</sup>, Y<sup>3+</sup>, La<sup>3+</sup>, Gd<sup>3+</sup>, and Sm<sup>3+</sup>) and dopant concentration [1–4]. It is generally accepted that Gd<sup>3+</sup>- or Sm<sup>3+</sup>-doped ceria exhibits the highest conductivity due to the small association enthalpy between

dopant cation and oxygen vacancy in the fluorite lattice [5,6].

To develop electrolytes for SOFC applications, studies of the sintering and microstructure of electrolytes are important for obtaining dense materials with higher ionic conductivity. It is noted that the sintering and densification behaviour of ceria-based electrolytes rely strongly on the characteristics of the raw powders (e.g., particle size and particle-size distribution) [7–11]. In this study, high-purity commercial CeO<sub>2</sub> and Gd<sub>2</sub>O<sub>3</sub> have been used as starting materials to form the oxide mixture (20% Gd<sub>2</sub>O<sub>3</sub> + 80% CeO<sub>2</sub>). The solubility of Gd<sub>2</sub>O<sub>3</sub> in CeO<sub>2</sub> has been carefully studied through measurements of the lattice parameter, instead of X-ray diffraction (XRD) reflection patterns. In addition, microstructural evolution, grain growth, and ionic conductivity have been also examined in the sintering temperature range of 1200–1700 °C.

## 2. Experimental procedure

High purity commercial CeO<sub>2</sub> (>99.5%) and Gd<sub>2</sub>O<sub>3</sub> (>99.9%) were used as starting materials. The SiO<sub>2</sub> impurities are around 74 and 86 mass ppm for the CeO<sub>2</sub> and Gd<sub>2</sub>O<sub>3</sub>

\* Corresponding author. Fax: +65-6790-0920.  
E-mail address: [tszhang@ntu.edu.sg](mailto:tszhang@ntu.edu.sg) (T.S. Zhang).

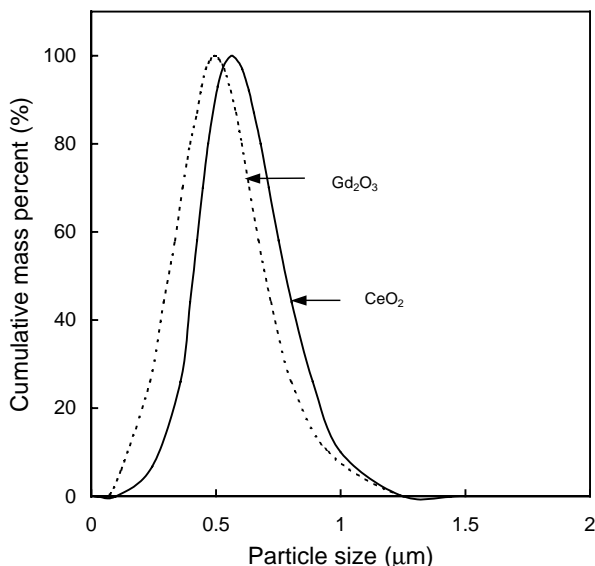


Fig. 1. Particle-size distribution of commercial  $\text{CeO}_2$  and  $\text{Gd}_2\text{O}_3$  powders.

powders, respectively. The particle-size distribution of the powders measured by means of a laser particle-size analyser (Analysette 22 Compact, Fritsch, Germany) are shown in Fig. 1. Both powders consist of mainly submicron-sized particles with mean diameters of  $\sim 0.55 \mu\text{m}$  ( $\text{CeO}_2$ ) and  $\sim 0.50 \mu\text{m}$  ( $\text{Gd}_2\text{O}_3$ ).

The  $\text{Ce}_{0.8}\text{Gd}_{0.2}\text{O}_{2-\delta}$  powder was prepared through a mixed-oxide method from the above oxides. The mixture was ground in ethanol by ball milling in polypropylene jars with yttria-stabilised zirconia balls for over 24 h. After drying, the mixture was pressed at  $\sim 100 \text{ MPa}$  into pellets using a stainless-steel die with a diameter of 10 mm. The green density was  $\sim 60\%$  of theoretical density. To prevent contamination during sintering, the pellets were supported with thin platinum plates, and were sintered at  $1200\text{--}1700^\circ\text{C}$  for 5 h in air, at heating and cooling rates of  $10^\circ\text{C}$  per minute. Some sintering experiments were performed using a dilatometer (Setsys 16/18, Setaram, France).

X-ray diffraction analysis was performed with a Rigaku (Dmax-2200, Tokyo, Japan) diffractometer that used  $\text{Cu K}\alpha$  radiation. A software package was used to determine the lattice parameters. The densities of the sintered pellets were measured by means of the Archimedes method in water bath. The microstructures were examined with scanning electron microscopy (SEM; JSM-5410, Oxford, UK). The grain size was determined using a linear intercept method by counting more than 250 grains in SEM micrographs. After polishing with fine emery papers, silver wires served as electrodes and silver paste was used to fix silver wires on to both sides of the pellets at  $850^\circ\text{C}$ . The ionic conductivities of the sintered pellets were measured from 250 to  $850^\circ\text{C}$  in air by two-probe impedance spectroscopy (Solartron, 1260, UK) from 1 to  $10^7 \text{ Hz}$ . A software package was used to separate the contributions of the grain interior (GI) and the grain boundary (GB) to the total conductivity.

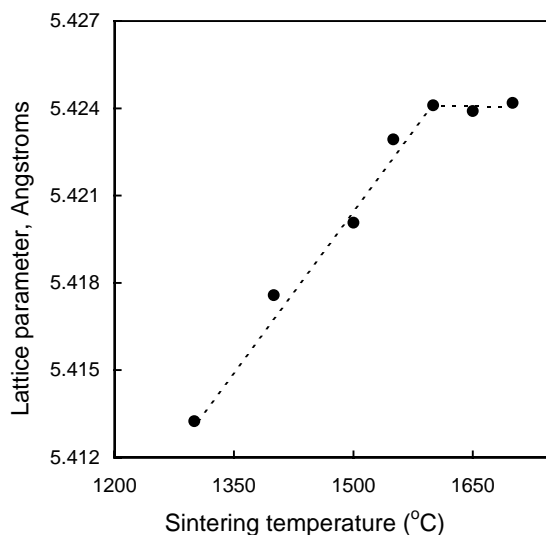


Fig. 2. Lattice parameter vs. sintering temperature for 5 h of 20%  $\text{Gd}_2\text{O}_3$ -doped  $\text{CeO}_2$ .

### 3. Results and discussion

#### 3.1. X-ray diffraction analysis

The lattice parameter is shown in Fig. 2 as a function of the sintering temperature for 20%  $\text{Gd}_2\text{O}_3$ -doped ceria ceramics. Beginning with the mixture of  $\text{CeO}_2$  and  $\text{Gd}_2\text{O}_3$ , the lattice constant increases with increasing sintering temperature and reaches a maximum at  $1600^\circ\text{C}$ . It remains almost unchanged at higher temperatures. The increase in the lattice constant with sintering temperature below  $1600^\circ\text{C}$  is due to the dissolution of  $\text{Gd}_2\text{O}_3$  in  $\text{CeO}_2$  since  $\text{Gd}^{3+}$  ions have a larger radius ( $1.05 \text{ \AA}$ ) than  $\text{Ce}^{4+}$  ions ( $0.97 \text{ \AA}$ ). A maximum lattice constant at  $1600^\circ\text{C}$  actually implies completion of the dissolution of  $\text{Gd}_2\text{O}_3$  in  $\text{CeO}_2$ . This also suggests that a sintering temperature of  $1600^\circ\text{C}$  is sufficiently high to ensure the dissolution of  $\text{Gd}_2\text{O}_3$  into  $\text{CeO}_2$  to form ceria-based solid solutions.

It should be pointed out that the development of the C-type structure of  $\text{Gd}_2\text{O}_3$  in  $\text{CeO}_2$  cannot be clearly observed from the XRD patterns since the reflections overlap heavily due to the close relationship between the C-type and fluorite structures. In the present work, the phase of  $\text{Gd}_2\text{O}_3$  cannot be identified from the mixture (20%  $\text{Gd}_2\text{O}_3$  + 80%  $\text{CeO}_2$ ) sintered above  $1300^\circ\text{C}$ . The results in Fig. 2, however, clearly show that the dissolution of  $\text{Gd}_2\text{O}_3$  in  $\text{CeO}_2$  below  $1600^\circ\text{C}$  is far from completion. Therefore, it is not reliable to judge the formation of ceria-based solid solutions from XRD reflection patterns alone.

#### 3.2. Sintering behaviour and microstructure

The linear shrinkage rate as a function of temperature for undoped and 20% Gd-doped samples is given in Fig. 3. The temperature of the maximum shrinkage rate ( $T_{\text{Max}}$ ) increases

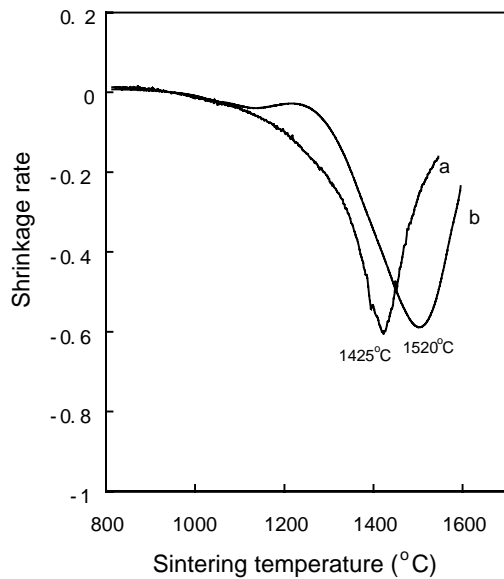


Fig. 3. Effect of sintering temperature (at a heating rate of  $10^{\circ}\text{C}$  per minute) on shrinkage rate for: (a) undoped and (b) 20%  $\text{Gd}_2\text{O}_3$ -doped  $\text{CeO}_2$  ceramics.

from  $\sim 1425^{\circ}\text{C}$  for undoped  $\text{CeO}_2$  to  $\sim 1520^{\circ}\text{C}$  for 20% Gd-doped  $\text{CeO}_2$ . This suggests that Gd doping increases the sintering temperature and retards the densification of ceria ceramic.

The microstructural evolution of 20% Gd-doped samples in the temperature range of  $1300$ – $1700^{\circ}\text{C}$  is shown in Fig. 4. The sample sintered at  $1300^{\circ}\text{C}$  for 5 h is very porous (with only  $\sim 73\%$  relative density), see Fig. 4(a). The pores are found to be continuous and open, and there is no significant grain growth. With increase in sintering temperature, the sintered density increases. A relative density of about 92% is achieved at  $1500^{\circ}\text{C}$ ; the pores in the sample (Fig. 4(c)) are closed and isolated, but the grain growth is still less pronounced. Large grains are present in some regions (Fig. 4(d)), which demonstrates the inhomogeneity of Gd distribution. This is because gadolinia has a tendency to suppress the grain growth of  $\text{CeO}_2$  [4]. The large grains, which usually contain a relatively small amount of gadolinia, disappear as the temperature is increased further. After sintering at  $1600$ – $1700^{\circ}\text{C}$ , the samples (Fig. 4(e) and (f)) display a uniform grain-size distribution. Moreover, at all the temperatures used, no intra-granular pores are observed. Only one type of pore close to the larger grains is identified, and is located at the grain boundaries or at the triple points. These closed pores can be readily eliminated from the sintered samples at high sintering temperatures as can be clearly seen in Fig. 4(e) and (f).

The effect of sintering temperature on the density and grain size of the undoped and doped samples sintered at  $1200$ – $1700^{\circ}\text{C}$  for 5 h is presented in Fig. 5. It is noted that under the same sintering conditions, the undoped  $\text{CeO}_2$  has a higher sintered density than the doped sample, which agrees well with the dilatometry measurements (Fig. 2). It

is also found that the grain growth of pure  $\text{CeO}_2$  is more rapid than that of Gd-doped samples, especially in the higher temperature range (e.g.,  $>1600^{\circ}\text{C}$ ). For example, at  $1670^{\circ}\text{C}$ , the mean grain size of pure  $\text{CeO}_2$  is  $\sim 30\ \mu\text{m}$ , but is only  $\sim 10.5\ \mu\text{m}$  at  $1700^{\circ}\text{C}$  for Gd-doped  $\text{CeO}_2$ . This indicates that Gd addition also depresses the grain growth of  $\text{CeO}_2$ .

### 3.3. Electrical properties

The ionic conductivity of  $\text{Ce}_{0.8}\text{Gd}_{0.2}\text{O}_{2-\delta}$  ceramics was measured by means of two-probe impedance spectroscopy. The interpretation of impedance data for polycrystalline materials, such as yttria-stabilised zirconia, has been well documented [12,13]. The ac impedance of an ionic conductor measured via a two-probe method contains contributions from the grain interior, the grain boundaries and the electrode–electrolyte interfaces. These can be represented in a complex plane by three successive arcs. In a practical case, however, not all these three arcs are observed, as dictated by the nature of the sample and the measurement conditions. In the present case, the three arcs can be identified clearly at a lower temperature (usually  $\leq 400^{\circ}\text{C}$ ), as shown in Fig. 6. Ionic conductivities (i.e., grain interior ( $\sigma_{\text{gi}}$ ), grain boundary ( $\sigma_{\text{gb}}$ ), and total ( $\sigma_{\text{t}}$ ) conductivities) of  $\text{Ce}_{0.8}\text{Gd}_{0.2}\text{O}_{2-\delta}$  can be obtained by fitting the impedance data by means of a software package.

The effect of sintering temperature on the GI, GB and total conductivities of  $\text{Ce}_{0.8}\text{Gd}_{0.2}\text{O}_{2-\delta}$  ceramics is presented in Fig. 7. The GB conductivity reaches a maximum at  $\sim 1550^{\circ}\text{C}$ , but the GI has a maximum conductivity at  $\sim 1600^{\circ}\text{C}$ . It is widely accepted that  $\text{SiO}_2$  impurity is a major factor responsible for the GB behaviour, and that the  $\text{SiO}_2$  originates mainly from precursor chemicals and ceramic processing. A thin Si-rich film is formed during sintering, and this blocks the movement of oxygen vacancies across the grain boundaries. In the present study, however, the lower GB conductivity below  $1550^{\circ}\text{C}$  should not be attributed solely to an intergranular siliceous phase. Rather, inhomogeneous distribution of gadolinium, which also blocks the movement of oxygen vacancies, may play a major role in the deteriorated GB behaviour of the sample. From the lattice measurement shown in Fig. 2, it is evident that a certain amount of gadolinium is still outside the lattice of ceria in samples sintered below  $1550^{\circ}\text{C}$ , and is most probably located at the grain boundaries. The maximum GB conductivity at  $1550^{\circ}\text{C}$  should be attributed to small grain size as well as to a more homogeneous distribution of gadolinium as compared with samples sintered below  $1550^{\circ}\text{C}$ . The sample sintered at  $1550^{\circ}\text{C}$  also has the lowest activation energy for GB conduction, as listed in Table 1. Although the segregation of gadolinium at the grain boundaries becomes less important as the sintering temperature is taken above  $1550^{\circ}\text{C}$ , a higher sintering temperature leads to rapid grain growth. Moreover, a high temperature is also helpful in promoting further propagation of  $\text{SiO}_2$  along grain boundaries. As a result, above

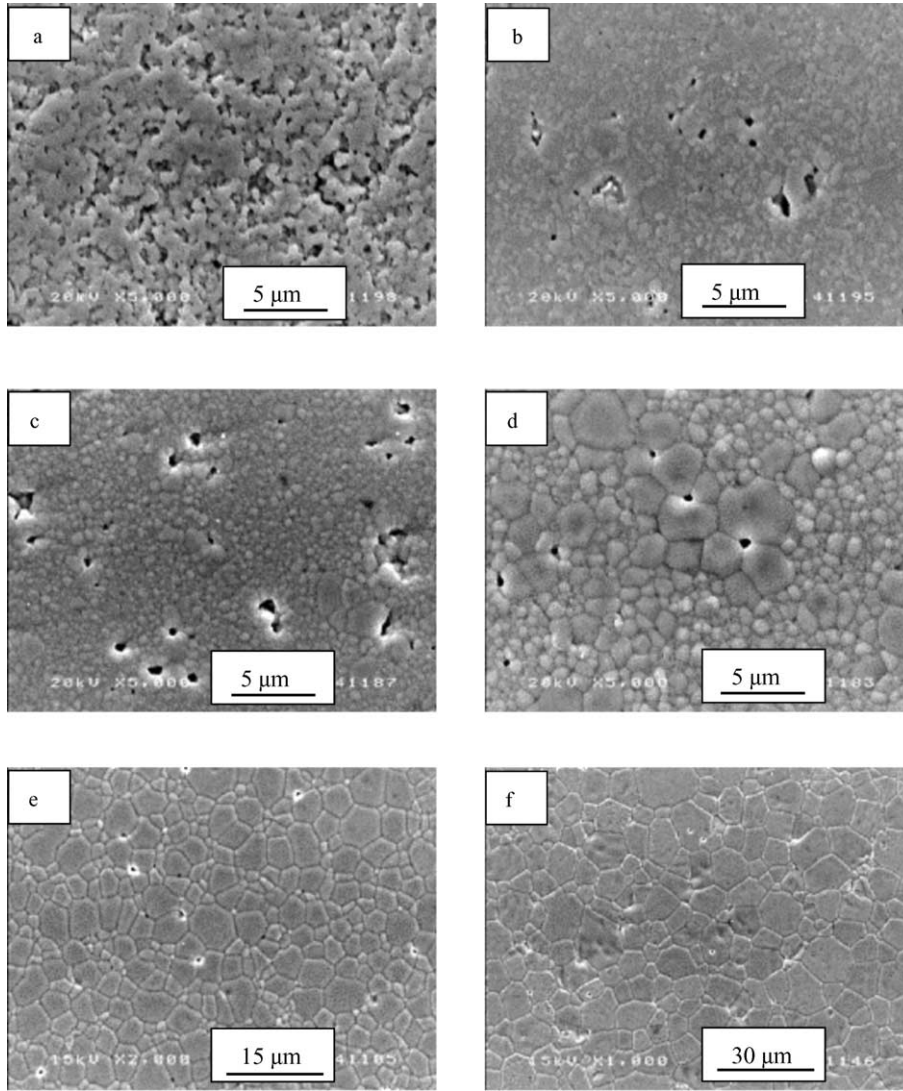


Fig. 4. Electron micrographs of 20%  $\text{Gd}_2\text{O}_3$ -doped  $\text{CeO}_2$  sintered in air for 5 h at (a) 1300 °C, (b) 1400 °C, (c) 1500 °C, (d) 1550 °C, (e) 1600 °C and (f) 1700 °C.

1550 °C, the GB conductivity decreases as the temperature increases.

From the data in Fig. 2, it is easy to understand why the GI conductivity reaches a maximum at 1600 °C since the

dissolution of gadolinia in ceria is completed at this temperature. Accordingly, the lowest activation energy for GI conduction is also obtained for the  $\text{Ce}_{0.8}\text{Gd}_{0.2}\text{O}_{2-\delta}$  ceramic sintered at 1600 °C, see Table 1. On the other hand, further

Table 1  
Sintering temperature, ionic conductivity and activation energy of  $\text{Ce}_{0.8}\text{Gd}_{0.2}\text{O}_{2-\delta}$  ceramics

Sintering temperature (°C)	$\sigma_{\text{t}(750)} (\Omega\text{m})^{-1}$	$\sigma_{\text{t}(350)} (\Omega\text{m})^{-1}$	$\sigma_{\text{gi}(350)} (\Omega\text{m})^{-1}$	$\sigma_{\text{gb}(350)} (\Omega\text{m})^{-1}$	$E_{\text{a}}$ (eV)	$E_{\text{gi}}$ (eV)	$E_{\text{gb}}$ (eV)
1700	4.68	$3.45 \times 10^{-2}$	$2.60 \times 10^{-2}$	$8.54 \times 10^{-3}$	0.998	0.909	1.047
1650	5.79	$4.43 \times 10^{-2}$	$2.82 \times 10^{-2}$	$1.61 \times 10^{-2}$	0.964	0.907	1.037
1600	6.14	$6.62 \times 10^{-2}$	$3.95 \times 10^{-2}$	$2.67 \times 10^{-2}$	0.915	0.883	1.018
1550	4.96	$6.72 \times 10^{-2}$	$2.56 \times 10^{-2}$	$4.16 \times 10^{-2}$	0.920	0.970	1.012
1500	2.5	$1.64 \times 10^{-2}$	$5.92 \times 10^{-3}$	$1.05 \times 10^{-2}$	0.986	0.978	1.028
1450	1.19				1.105		

GB and GI conductivities measured at 350 °C, and total conductivity measured at 350 and 750 °C, respectively.  $E_{\text{a}}$  is the activation energy for total conductivity in temperature range of 250–850 °C.  $E_{\text{gi}}$  and  $E_{\text{gb}}$  are the activation energies for the GI and GB conductivities, respectively, in temperature range of 250–500 °C.

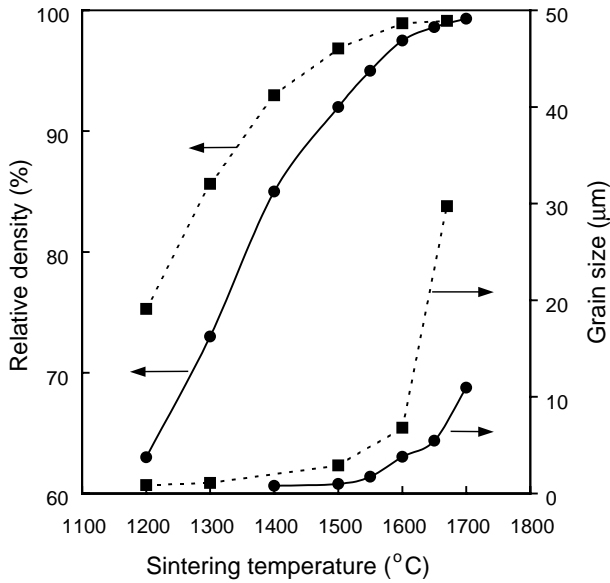


Fig. 5. Effect of sintering temperature for 5 h on sintered density and grain size of (■) undoped and (●) 20% Gd<sub>2</sub>O<sub>3</sub>-doped CeO<sub>2</sub> ceramics.

increase in temperature leads to a decrease in the GI conductivity as well as an increase in activation energy for GI conduction (Table 1). This should be attributed to the dissolution of SiO<sub>2</sub> into ceria solid solutions. At a higher sintering temperature, a small quantity of SiO<sub>2</sub> can be dissolved into Ce<sub>0.8</sub>Gd<sub>0.2</sub>O<sub>2-δ</sub> ceramic at either substitutional sites or interstitial sites, i.e.,

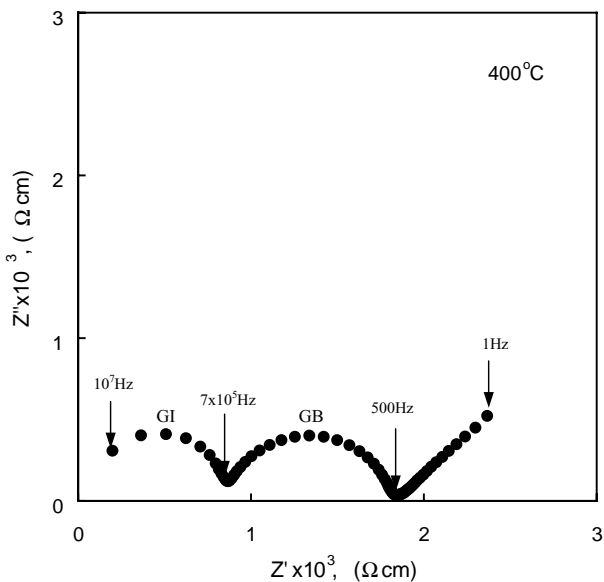
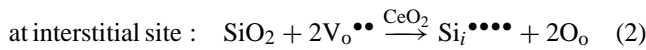
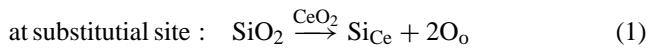


Fig. 6. Impedance plot of Ce<sub>0.8</sub>Gd<sub>0.2</sub>O<sub>2-δ</sub> ceramic sintered at 1600 °C for 5 h in air. Data were taken at 400 °C in air. GI and GB stand; respectively, for grain interior and grain boundary effects.

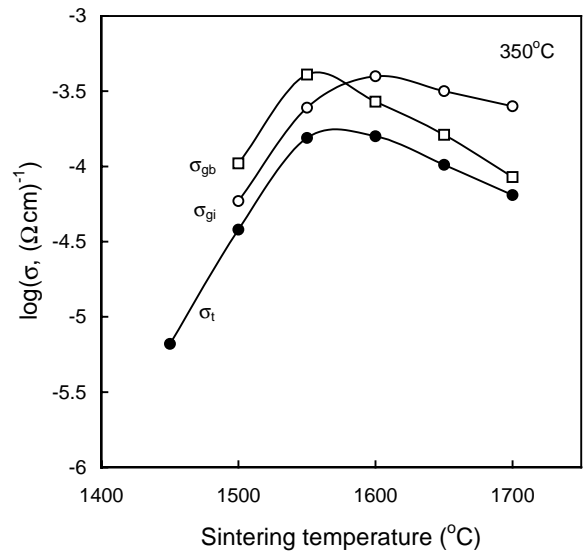


Fig. 7. Effect of sintering temperature on GI (σ<sub>gi</sub>), GB (σ<sub>gb</sub>), and total (σ<sub>t</sub>) conductivities of Ce<sub>0.8</sub>Gd<sub>0.2</sub>O<sub>2-δ</sub> ceramics, taken at 350 °C in air.

Although the dissolution of SiO<sub>2</sub> into Ce<sub>0.8</sub>Gd<sub>0.2</sub>O<sub>2-δ</sub> at substitutional sites produces no charge carriers as described in Eq. (1), a large lattice distortion usually leads to a slow mobility of oxygen vacancies, as well as to a high association enthalpy of complex defects. Similar results have been found in Zr-doped Ce<sub>0.75</sub>Gd<sub>0.15</sub>O<sub>2-δ</sub> by Zhang et al. [14], and in Al-doped YSZ by Feighery and Irvine [15]. By referring to the size of the Si<sup>4+</sup> ion (0.4 Å) and the Ce<sup>4+</sup> ion (0.97 Å), however, the interstitial dissolution of SiO<sub>2</sub> in Ce<sub>0.8</sub>Gd<sub>0.2</sub>O<sub>2-δ</sub> by filling some oxygen vacancies is more favourable, as described in Eq. (2). This results in a decrease in the concentration of oxygen vacancies, and thus reduces the GI conductivity.

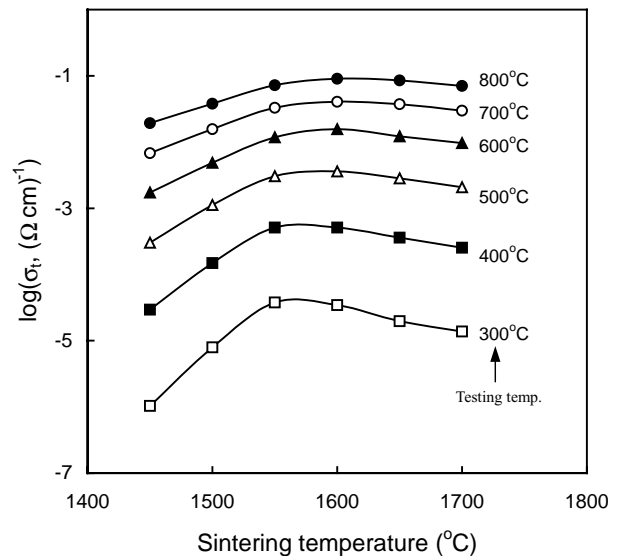


Fig. 8. Isothermal total conductivity of Ce<sub>0.8</sub>Gd<sub>0.2</sub>O<sub>2-δ</sub> ceramics sintered at different temperatures for 5 h in air.

The dependence of isothermal total conductivity on sintering temperature is shown in Fig. 8. It is noted that the maximum total conductivity shifts with the test temperature. Below 500 °C, the sample sintered at 1550 °C has a maximum total conductivity, followed by the samples with sintering temperatures at 1600, 1650, 1700 and 1500 °C. Above 500 °C, however, the total conductivity based on sintering temperature, decrease in the order: 1600, 1650, 1550, 1700 and 1500 °C. This can be also clearly identified from the results in Table 1. Inspection of the results in Fig. 7 suggests that below 500 °C, the maximum GB conductivity is responsible for the highest total conductivity of the sample sintered at 1550 °C. With increasing testing temperature, however, the GB effect gradually becomes less important. The total conductivity is mainly dominated by GI conduction. Therefore, above 500 °C, the sample sintered at 1600 °C has a highest total conductivity due to its highest GI conductivity among all the samples used. The above results suggest that the optimum sintering temperature range is between 1550 and 1600 °C.

#### 4. Summary

The development of the C-type structure of Gd<sub>2</sub>O<sub>3</sub> in CeO<sub>2</sub> cannot be clearly observed from XRD reflection patterns due to the close relationship between the C-type and fluorite structures. The dissolution of Gd<sub>2</sub>O<sub>3</sub> in CeO<sub>2</sub> is examined based on the measurements of the lattice parameter. It is found that the dissolution of Gd<sub>2</sub>O<sub>3</sub> in CeO<sub>2</sub> is completed at 1600 °C for 5 h.

The Gd doping increases the sintering temperature, and depresses the grain growth. At all temperatures from 1200 to 1700 °C, only a few intra-granular pores are observed;

almost all the pores are located at the grain boundaries or at the triple points. These pores can be readily eliminated from the sintered pellets at higher sintering temperatures (e.g., ≥1600 °C). Over 97% relative density is obtained for samples sintered at 1600 °C or above.

The sintering temperature has a significant effect on both the grain boundary and the grain interior conductivities, and thus on the total conductivity. The optimum sintering temperature range is found to be between 1550 and 1600 °C, in which the best electrical properties are achieved for 20% Gd-doped ceria solid solution.

#### References

- [1] D.Y. Wang, D.S. Park, J. Griffith, A.S. Nowick, *Solid State Ionics* 2 (1981) 95.
- [2] G.B. Balazs, R.S. Glass, *Solid State Ionics* 76 (1995) 155.
- [3] C. Tian, S.W. Chan, *Solid State Ionics* 134 (2000) 89.
- [4] T.S. Zhang, P. Hing, H.T. Huang, J.A. Kilner, *Solid State Ionics* 148 (2002) 567.
- [5] R. Gerhard-Anderson, A.S. Nowick, *Solid State Ionics* 5 (1981) 547.
- [6] J.A. Kilner, *Solid State Ionics* 8 (1983) 201.
- [7] H. Inaba, T. NakaJima, *Solid State Ionics* 106 (1998) 263.
- [8] A. Overs, I. Riess, *J. Am. Ceram. Soc.* 65 (1982) 606.
- [9] I. Riess, D. Braunshtein, D.S. Tannhauser, *J. Am. Ceram. Soc.* 64 (1981) 480.
- [10] R.S. Torrens, N.M. Sammes, G.A. Tompsett, *Solid State Ionics* 111 (1998) 9.
- [11] P.L. Chen, I.W. Chen, *J. Am. Ceram. Soc.* 80 (1997) 637.
- [12] J.E. Bauerle, *J. Phys. Chem. Solids* 30 (1969) 2651.
- [13] J.R. Macdonald (Ed.), *Impedance Spectroscopy—Emphasizing Solid Materials and Systems*, A Wiley/Interscience Publication, John Wiley & Sons, New York, 1987.
- [14] T.S. Zhang, H.T. Huang, Z.Q. Qiang, P. Hing, J.A. Kilner, *J. Mater. Sci. Lett.* 21 (2002) 1167.
- [15] A.J. Feighery, J.T.S. Irvine, *Solid State Ionics* 121 (1999) 47.